

Contrasting the Excited-State Dynamics of the Photoactive Yellow Protein Chromophore: Protein versus Solvent Environments

Mikas Vengris,* Michael A. van der Horst,[†] Goran Zgrablić,[‡] Ivo H. M. van Stokkum,* Stefan Haacke,[‡] Majed Chergui,[‡] Klaas J. Hellingwerf,[†] Rienk van Grondelle,* and Delmar S. Larsen*

*Faculty of Sciences, Vrije Universiteit Amsterdam, Amsterdam, The Netherlands; [†]Department of Microbiology, Swammerdam Institute for Life Sciences, University of Amsterdam, Amsterdam, The Netherlands; and [‡]Laboratoire de Spectroscopie Ultrarapide, Ecole Polytechnique Fédérale de Lausanne, Lausanne, Switzerland

ABSTRACT Wavelength- and time-resolved fluorescence experiments have been performed on the photoactive yellow protein, the E46Q mutant, the hybrids of these proteins containing a nonisomerizing “locked” chromophore, and the native and locked chromophores in aqueous solution. The ultrafast dynamics of these six systems is compared and spectral signatures of isomerization and solvation are discussed. We find that the ultrafast red-shifting of fluorescence is associated mostly with solvation dynamics, whereas isomerization manifests itself as quenching of fluorescence. The observed multiexponential quenching of the protein samples differs from the single-exponential lifetimes of the chromophores in solution. The locked chromophore in the protein environment decays faster than in solution. This is due to additional channels of excited-state energy dissipation via the covalent and hydrogen bonds with the protein environment. The observed large dispersion of quenching timescales observed in the protein samples that contain the native pigment favors both an inhomogeneous model and an excited-state barrier for isomerization.

INTRODUCTION

Photoactive yellow protein (PYP) is a water-soluble photoreceptor protein responsible for the negative blue-light-induced phototaxis of the halophilic phototropic bacterium, *Halorhodospira halophila* (Sprenger et al., 1993). This small 125-residue protein contains a *p*-coumaric acid chromophore that is covalently bound to the protein backbone via a thiol-ester cysteine linkage Cys-69 (Baca et al., 1994; van Beeumen et al., 1993). Upon photoexcitation, a complex photocycle is initiated within the protein, which ultimately triggers directed bacterial migration. These photocycle events occur over 14 orders of magnitude in time and include the isomerization and protonation of the chromophore, in addition to a partial unfolding (and refolding) of the protein (Cusanovich and Meyer, 2003; Hellingwerf et al., 2003; van Brederode et al., 1996). This partially unfolded state is the presumed signaling state for the photocycle and recovers back to the ground-state structure on an ~500-ms timescale (Genick et al., 1997; Rubinstenn et al., 1998).

Due to its ease of genetic manipulation and excellent photo- and chemical stability, PYP is an attractive model system for investigating photoreceptor protein responses. Time-resolved x-ray crystallography and Fourier-transform infrared spectroscopy have shown that extensive structural changes of both the chromophore and surrounding protein

occur during the photocycle (Genick et al., 1997; Perman et al., 1998; Ren et al., 2001; Xie et al., 2001), whereas pump-probe (Baltuška et al., 1997; Devanathan et al., 2000, 1999; Gensch et al., 2002; Larsen et al., 2004b) and time-resolved fluorescence (Changenet et al., 1998; Hanada et al., 2001; Mataga et al., 2000a, 2003) experiments have helped to identify the spectral and temporal properties of the photocycle intermediates. These studies and recent femto-second mid-IR experiments (Groot et al., 2003) have shown that the ultrafast (<10 ps) quenching of the PYP excited state is directly connected to the photoisomerization of the bound chromophore. Recently, several ultrafast dynamic studies on model PYP chromophores in solution have been performed (Changenet-Barret et al., 2002, 2001), including dispersed pump-probe (Larsen et al., 2003) and pump-dump-probe experiments (Larsen et al., 2004b).

A primary goal in investigating the photophysics of PYP, and photoreceptors in general, is to build a microscopic picture of how the photocycle is initiated, including effects from the inherent dynamics of the excited PYP chromophore and the resulting responses from the surrounding protein environment. The characterization of the potential energy surfaces involved in the photoinduced reactions is an important part of this picture, because these surfaces ultimately determine the driving force for the excited- and ground-state evolutions. An intriguing question about the photocycle of PYP is whether an energy barrier is hindering the excited-state photoisomerization process, which has been a matter of discussion for the bacteriorhodopsin (bR) photoreceptor (Gai et al., 1998, 1997; Gonzalez-Luque et al., 2000; Humphrey et al., 1998). The three-state model, which includes a small excited-state energy barrier (Fig. 1

Submitted March 19, 2004, and accepted for publication May 26, 2004.

Address reprint requests to Delmar S. Larsen, Fax: 31-0-20-444-7999; E-mail: dslarsen@nat.vu.nl.

Delmar S. Larsen's present address is Dept. of Chemistry, University of Southern California, Los Angeles, CA 90089.

© 2004 by the Biophysical Society

0006-3495/04/09/1848/10 \$2.00

doi: 10.1529/biophysj.104.043224

B), was favored over a two-state barrierless model (Fig. 1 A). In the case of a barrierless two-state model (Fig. 1 A), a dynamic red-shift of the stimulated emission or fluorescence should be observed as the system evolves on the excited-state potential and the energy gap between the ground and excited state decreases. However, for bR, such a red-shift was not observed (Du and Fleming, 1993; Hasson et al., 1996). The fluorescence lifetime should be largely temperature-independent; however, a pronounced temperature-dependence has been observed for bR (Alfano et al., 1976). These observations have been combined into a self-consistent picture of the photoreaction pathway in bR (Gai et al., 1998). However, based on recent quantum chemical calculations, the issue of an excited-state barrier is not unambiguously solved for bR, and a two-state/two-mode model seems to describe the experimental observations equally well (Gonzalez-Luque et al., 2000). The collection of time-resolved fluorescence spectra is insightful for the investigation of the excited- and ground-state potential energy surfaces along the photoreaction coordinates.

For bR, the stimulated emission spectrum does not resemble its fluorescence spectrum, indicating that excited-state absorption partially overlaps the stimulated emission, which was further supported by the measured power dependence of pump-dump-probe signals (Gai et al., 1998, 1997). This emphasizes the aspect that pump-probe signals inherently include overlapping contributions from multiple origins, including excited-state, ground-state, and product-state absorptions, in addition to ground-state bleach and stimulated emission. In contrast, fluorescence measurements are sensitive only to excited-state dynamics, and other interfering contributions are simply excluded. Even though no clearly resolvable excited-state absorption bands have been observed that overlap the stimulated emission band in PYP, the initial intermediates of the photocycle certainly do (Baltuška et al., 1997; Devanathan et al., 2000; Imamoto et al., 2001). Consequently, measuring the time-resolved fluorescence is useful in characterizing the excited-state dynamics of the PYP system.

In this study, we explore these dynamics with a novel time- and wavelength-resolved fluorescence up-conversion technique that builds on the single wavelength measurements used

successfully for investigating solvation and photoreaction dynamics (Changenet et al., 1998; Du and Fleming, 1993; Jimenez et al., 1994; Mataga et al., 2000b). This article outlines the results of investigating the excited-state dynamics of six different PYP-related systems: two isolated model PYP chromophores in solution and four PYP protein samples (Fig. 2). The two isolated chromophores in solution: thiomethyl *p*-coumaric acid (TMpCA) and 7-hydroxy-coumarin-3-carboxylic acid, which is referred to here as the free-acid-locked (FAL) analog, share similar spectroscopic and structural features. A rich set of dynamics has been observed in TMpCA (Larsen et al., 2003, 2004a), that are similar to the spectroscopic properties of the WT PYP system (Devanathan et al., 1999; Gensch et al., 2002), justifying the use of this chromophore as a model for investigating the inherent PYP chromophore dynamics independent of the protein environment. The TMpCA chromophore is free to rotate around its C4–C7 and C7=C8 dihedral angles, and excited-state quenching is determined by the photoreaction of twisting (or isomerization). However, in FAL, the possibility of isomerization is excluded by the additional covalent bonds, which results in an excited-state lifetime that is three orders-of-magnitude longer than for TMpCA. Attaching a thioester group to FAL shifts the absorption spectrum of the compound to the red by 34 nm (420 nm for the thioester versus 386 nm for FAL); however, the ultrafast dynamics from the pump-probe techniques is not significantly altered (Larsen et al., 2004a; M. Vengris, M. A. van der Horst, K. J. Hellingwerf, R. van Grondelle, and D. S. Larsen, unpublished)—the compound behaves essentially as a fluorescent dye molecule in solution, exhibiting a >2-ns excited-state lifetime, with <2-ps solvation dynamics. Because of this similarity, in this study we selected the commercially available FAL sample in lieu of the thio-methylated FAL sample. The four protein samples that were studied include the native chromophore in both the wild-type PYP environment (WT PYP) and its E46Q mutant, where the hydrogen-bonding glutamic acid residue at position 46 is mutated into a weaker hydrogen-bonding glutamine (Fig. 2 C). The two other studied protein systems are the WT and E46Q proteins with the locked chromophore substituted for the native one (WTL and E46QL, respectively). The comparison between locked and native chromophore (both

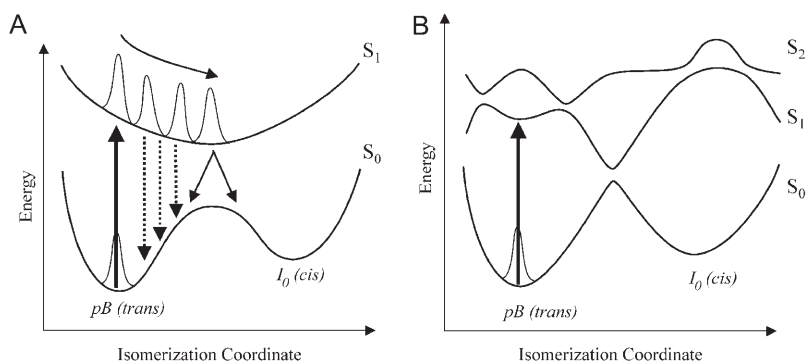


FIGURE 1 Suggested ground- and excited-state potential energy curves for the isomerization reaction of the PYP chromophore. (A) Two-state barrierless isomerization model. Excited- and ground-state evolution is depicted by solid arrows. The dashed arrows illustrate the dynamic red-shift of fluorescence expected for this mechanism. (B) Three-state model with a small barrier in the excited state.

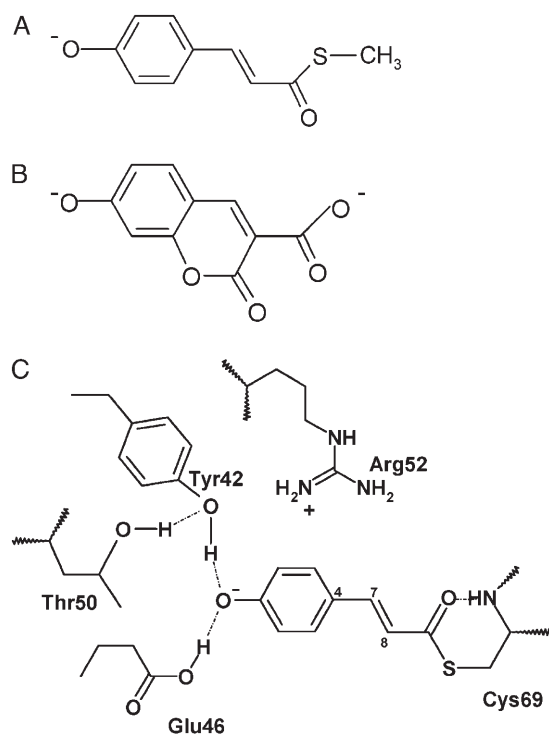


FIGURE 2 PYP chromophore structures. (A) TMpCA, (B) FAL, and (C) Chromophore binding pocket in WT PYP with the native chromophore. Isolated chromophores are shown at high pH with the phenolic group deprotonated.

inside the proteins and in solution) signals allow us to explore the role of isomerization in the excited-state dynamics. Moreover, contrasting the observations on the pigments in solution versus protein matrix allows us to separate the effects arising from the protein matrix from those inherent to the chromophores.

EXPERIMENT

ApoPYP was produced and isolated as a hexahistidine-tagged apo-protein in *Escherichia coli* and was reconstituted with the 1,1-carbonyldiimidazole derivative of the *p*-coumaric acid chromophore (Kort et al., 1996). Protein samples were used without removal of their hexahistidine-containing N-terminal tag in 10 mM Tris/HCl, pH = 8. TMpCA was chemically synthesized as described in Larsen et al. (2004a) from *p*-coumaric acid (Aldrich, St. Louis, MO), whereas FAL (7-hydroxycoumarin-3-carboxylic acid) was directly purchased (Molecular Probes, Eugene, OR). Both free chromophores were studied in an aqueous alkaline buffer (10 mM CAPS) with a pH of 10.5. The high pH best simulates the environment found for the chromophore in the native PYP protein, where the phenolic moiety of the chromophore is deprotonated (Cusanovich and Meyer, 2003; Kort et al., 1998). The absorption spectra of the samples were measured before and after data collection and no significant changes were observed.

The fluorescence signals were collected with a novel homebuilt, broadband up-conversion setup, which is briefly outlined below (Haacke et al., 1998; Zgrablić et al., 2003). A Ti:Sapphire amplified laser system (Mira/RegA, Coherent, Santa Clara, CA) was used to generate 50-fs (full width at half-maximum, FWHM) 800-nm laser pulses with a 250-kHz repetition rate. Approximately 10% of the amplified beam was used as a gate pulse, and was controlled with a 0.1-μm resolution mechanical delay line (Newport, Irvine, CA). The rest was frequency-doubled in a 0.5-mm-thick β-barium borate

nonlinear crystal and used as 400-nm excitation light (~22 nJ/pulse). These pulses were focused (~60-μm FWHM spot size) onto a 0.5-mm-pathlength flow cell with the samples circulating at a 1.5 ml/s rate. The emitted fluorescence was then collimated and focused with off-axis parabolic reflectors (Janos Optics, Townshend, VT) with the focal distances of 50 and 225 mm, respectively, into a second nonlinear crystal (250-μm-thick β-barium borate) with spatial and temporal overlap with the 800-nm gate pulse.

The resulting up-converted fluorescence light was dispersed in a spectrograph and collected using a liquid-nitrogen-cooled, back-illuminated charge-coupled device camera. A single time-gated spectrum was recorded by rotating the up-conversion crystal by 30° at a constant angular velocity (to ensure phase-matching across the whole spectral range of fluorescence) while accumulating the charge on the charge-coupled device chip (Haacke et al., 1998). The wavelength sensitivity was then calibrated with the known fluorescence spectrum of FAL. The setup had an instrument response function (IRF) of 190 fs FWHM with an ~3-nm wavelength resolution. The group velocity dispersion of the different spectral components has been characterized with a white-light spectrum generated from water in the above flow cell and all data presented here are corrected for the group velocity dispersion. The simultaneous collection of the complete fluorescence spectrum at each time point allows us to exclude the need of performing a spectral reconstitution procedure (Jarzeba et al., 1991) used for comparing multiple signal wavelength up-conversion traces.

The measured data was fitted using a sequential (evolutionary) multi-wavelength global analysis model (Hoff et al., 1994; Holzwarth, 1996), where different compartments, characterized by the concentrations $c_i(t)$, evolve in series ($c_1(t) \xrightarrow{\tau_1} c_2(t) \xrightarrow{\tau_2} \dots$). The time-dependent concentrations are described by the system of differential equations

$$\begin{aligned} \frac{dc_1(t)}{dt} &= I(t) - \frac{1}{\tau_1}c_1(t), \\ \frac{dc_i(t)}{dt} &= \frac{1}{\tau_{i-1}}c_{i-1}(t) - \frac{1}{\tau_i}c_i(t), i \neq 1, \end{aligned} \quad (1)$$

and the model function used to fit the fluorescence data is then

$$F(t, \lambda) = \sum_i c_i(t) \sigma_i(\lambda). \quad (2)$$

Here $\sigma_i(\lambda)$ is a species-associated emission spectrum (SAES) for the i^{th} component and $I(t)$ is the input in the system affecting only the first compartment, which has a Gaussian profile with the FWHM of IRF. Such analysis provides a convenient means of parameterizing the observed data into a set of spectra “evolving” into each other with sequentially decreasing lifetimes. This does not necessarily imply that the observed dynamics results from a sequential process, and can equally well describe a set of processes that evolve in parallel. For example, if a dynamic red-shifting of the fluorescence spectrum is observed in the sample, the estimated sequential SAES would all be positive with correspondingly shifted spectral maxima. Instead, if the same data were fitted using a parallel model with the same number of independent exponentially decaying compartments, the SAES would show a positive contribution (loss) at the blue side of the spectrum and a negative one (gain) in the red. In both cases, the estimated lifetimes would be exactly the same. Since fluorescence spectra are positive by definition, we opt for the sequential model because the resulting SAES are more intuitive to interpret.

RESULTS

Free chromophores

With the aid of global analysis, detailed information can be extracted from the measured fluorescence signals; however,

some informative properties can be gleaned from investigating the raw signals directly. Fig. 3 shows an overview of the signals collected for WT PYP and WTL proteins and the corresponding free chromophores in solution. The most obvious observation in these signals is that the fluorescence from the locked chromophores in the FAL and WTL samples extends beyond our instrumental time window (~ 100 ps), whereas the fluorescence from the native chromophores in the TMpCA and WT PYP samples are quenched on considerably faster timescales. These long excited-state lifetimes for the locked chromophores result from removing the twisting degree of freedom, and the enhanced internal conversion associated with it. Furthermore, the signal from the isolated chromophores in solution exhibits a time-dependent red-shift, which is not observable in the protein samples. It should be noted that in all samples, much of the dynamic Stokes shift occurs significantly faster than our IRF. In particular for the protein samples, the fluorescence spectra attain their steady-state spectral position on a timescale faster than the present time resolution, suggesting that an ultrafast intramolecular relaxation and/or dielectric solvation are operative.

Single-wavelength fluorescence traces measured at the respective fluorescence maxima are contrasted in Fig. 4 A. Whereas the TMpCA trace (*solid circles*) is almost completely quenched within 10 ps, the FAL trace (*open circles*) exhibits no appreciable decay within our time window. Fig. 5 shows a set of normalized, dispersion-corrected time-gated spectra measured between -80 and 120 fs with equal time steps for WT PYP, WTL, and TMpCA. In WT PYP, the narrowing of the spectra is observed during the first 100 fs (indicated by *arrows* in Fig. 5 A), whereas no significant

change is observed in WTL. In TMpCA (Fig. 5 C), a slight red-shifting and narrowing (see the enlargement in Fig. 5 *insets*) is observed in this time frame. Note that the region around 460 nm also contains contributions from Raman scattering in the water solvent. The time-profile of this Raman signal is limited to the IRF timescale and interferes with a observed ultrafast narrowing of the spectra.

In Fig. 6, the same data is presented in the form of kinetic traces along with the global analysis fit depicted by solid lines. The narrowing in WT PYP (Fig. 6 A) is observed as faster decays on the red (480 nm) and blue (555 nm) wings of the fluorescence spectrum in contrast to the fluorescence maximum (500 nm). At 480 nm, there is a slight contamination from the Raman scattering which results in the difference between the 480 -nm and 555 -nm traces. In WTL (Fig. 6 B), fluorescence traces at different parts of the emission spectrum exhibit essentially identical behavior during the first 2 ps (and beyond). No appreciable decay is observed in this time window (see also Fig. 4). In contrast, the TMpCA traces (Fig. 6 C) show a delayed rise at the red edge of the fluorescence spectrum occurring simultaneously with the decay of the blue wing of the band, which reconfirms the shifting behavior observed in Figs. 3 and 5.

This 2-ps time-dependent red-shifting is observed in both free chromophores (Fig. 3, C and D, and Fig. 5 C). The estimated SAES from the global analysis and corresponding timescales resulting from the sequential model fit to the TMpCA data are shown in Fig. 7 A; four components were required to obtain a satisfactory fit. The time constants are reliably estimated for the final three components, whereas the initial relaxation occurring within our 190-fs IRF was fixed at 100-fs. The dynamic red-shift is clearly observed

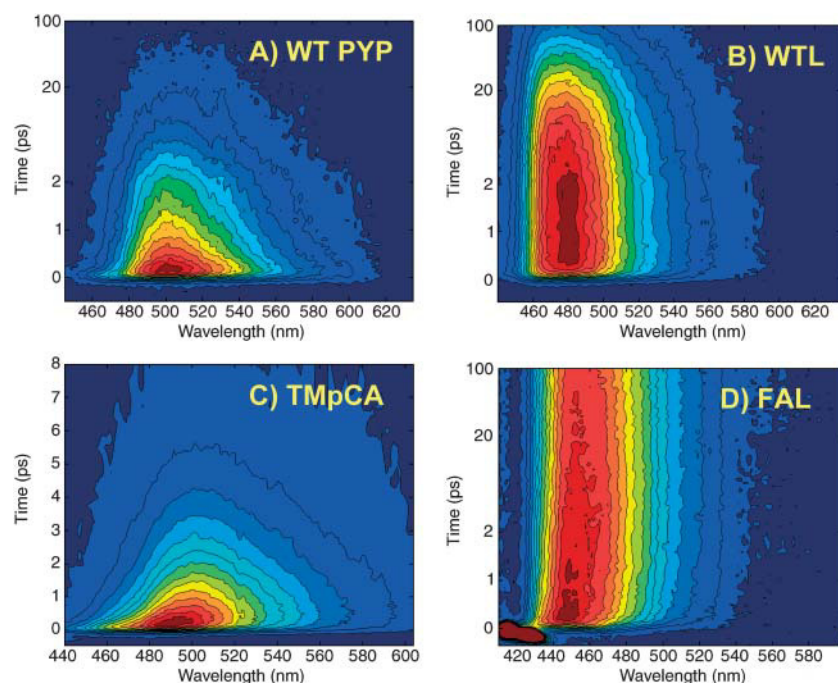


FIGURE 3 Dispersion-corrected wavelength- and time-resolved fluorescence signals of (A) WTPYP, (B) WTL, (C) TmpCA, and (D) FAL. The contour levels set at 6.7% of the maximum. Note different time axes.

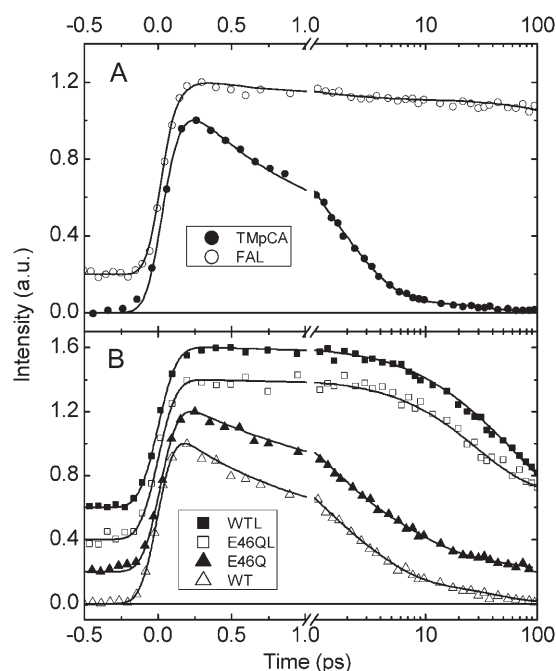


FIGURE 4 Fluorescence kinetics at the fluorescence maximum. (A) TMpCA (solid circles) and FAL (open circles) in solution; (B) WT PYP (open triangles), E46Q mutant (solid triangles), E46QL (open squares), and WTL (solid squares). The traces were normalized on the maximum value and offset by 0.2 for clarity. Solid lines show the global analysis fit to the data. Some time points were excluded to aid in viewing.

from the analysis by contrasting the early time SAES (#1 and #2) with the latter times SAES (#3 and #4). The Raman scattering feature from the solvent peaking around 460 nm is observed in the first SAES of all samples.

The shifting in TMpCA occurs on two characteristic timescales: one faster than our IRF (fixed to 100 fs), and 450 fs (the latter timescale also includes some decay). Concomitant with this shifting is a 2-ps decay, which quenches most of the fluorescence, except for a weak 30-ps component (#4) with a near-zero amplitude (which may be an experimental artifact due to incomplete background subtraction). Similar red-shifting is observed for FAL, but with slightly different time constants: 100 fs, 300 fs, and 1.8 ps. The decay time of FAL was estimated to be 1.4 ns, although the experimental window of these measurements (100 ps) limits an accurate estimate of this lifetime.

Protein signals

The protein signals are noticeably different from those of the free chromophores (Figs. 3, 5, and 6); the principal differences are that no clear spectral shifting is resolvable in the proteins and that the quenching timescales are distinctly multiexponential (i.e., the estimated time constants represent decays and not spectral shifts like in the isolated chromophores). The overall fluorescence decay is slightly slower in

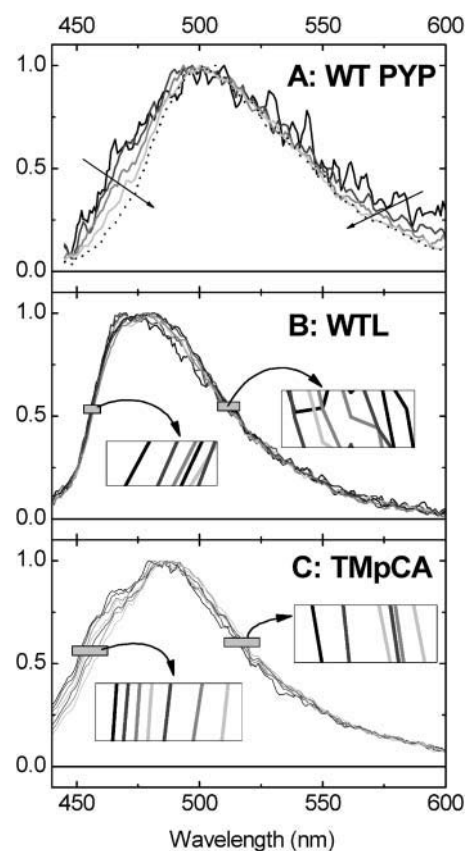


FIGURE 5 Time-gated fluorescence spectra measured on WT PYP (A), WTL (B), and TMpCA (C). The spectra have been corrected for group velocity dispersion and normalized at the peak. The delay times are from -80 fs to 120 fs, at equal time intervals. The arrows in A show the observed narrowing trend in WTPYP. The insets in B and C show a blowup of the data in the selected regions. In TMpCA, a shifting is observed (the consecutive spectra are cyclically coded in the grayscale levels from the darkest to the lightest), whereas FAL shows no clear trend. The relative signal amplitudes confirming the trends are shown in Fig. 6.

WT PYP than in the TMpCA in solution and considerably faster than in WTL (Fig. 4 B). Four lifetimes are estimated (Fig. 7 C): 100 fs, 750 fs, 3.3 ps, and 40 ps. The shapes of the last three SAES are essentially identical, although the initial one is slightly broader. As with WT PYP, the fluorescence evolution in WTL protein exhibits no spectral shifting (Figs. 3 B and 5 B). The fluorescence decay is considerably slower in WTL than in WT PYP; however, it is approximately an order-of-magnitude faster than in FAL (Fig. 4 A). Global analysis (Fig. 7 D) revealed two lifetimes: 13 ps and 72 ps (there is also a sub-IRF component—not shown—which accounts mostly for the Raman scattering). As with the WT PYP signals, the two SAES have near-identical spectral shapes (i.e., no spectral shifting dynamics occurs).

The fluorescence decay in the E46Q mutant resembles that of WT PYP (Fig. 4 B, and Fig. 7, C and D), albeit with slightly slower time constants. Again the only observed spectral evolution is a sub-ps narrowing of fluorescence spectrum. In the E46QL sample, the fluorescence decays

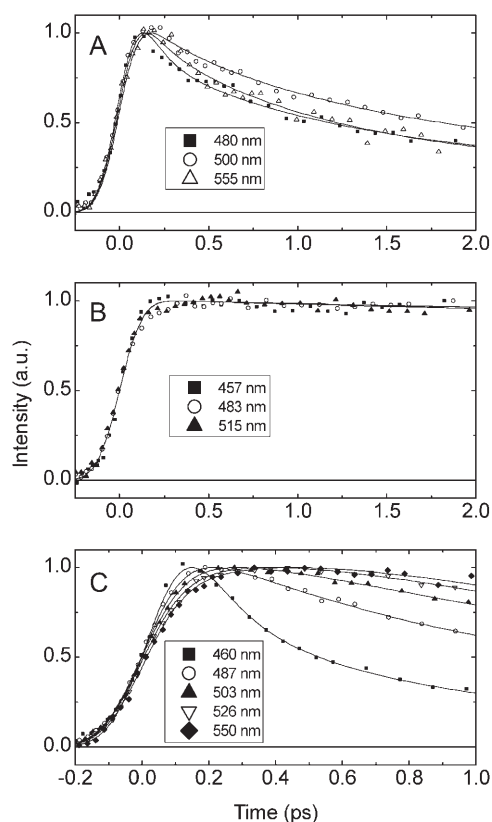


FIGURE 6 Time-resolved fluorescence traces measured in WT PYP (A), WTL (B), and TMpCA (C) at wavelengths shown in the legends. The traces have been corrected for group velocity dispersion and normalized. Solid lines show the sequential model fit to the data. The fit parameters are found in Fig. 7.

several times slower than in WTL (Fig. 7 F); the lifetimes are 25 and 430 ps.

DISCUSSION

Both free pigments in solution exhibit dynamic red-shift of fluorescence on a sub-2 ps timescale and since no twisting can occur in the locked chromophore, this shifting may be ascribed to either aqueous solvation or vibrational relaxation (Jimenez et al., 1994). The constructed Stokes-shift response functions describing the shifting dynamics irrespective of the signal amplitude,

$$S(t) = \frac{\bar{\nu}(t) - \bar{\nu}(\infty)}{\bar{\nu}(0) - \bar{\nu}(\infty)}, \quad (3)$$

for TMpCA and FAL are compared in Fig. 8, where $\bar{\nu}(t)$ is the first moment of the time-gated spectrum at time t . Both solvation curves can be fit with the same bi-exponential fitting function including 220 fs (50%) and 1 ps (50%) time constants and are comparable to the dynamics observed in similar aqueous solvation measurements (Jimenez et al.,

1994). The obtained time constants are different from the ones resulting from global analysis because only one aspect of the data (first moment) is analyzed and the total amount of data is greatly reduced (a three-dimensional time-resolved spectrum is projected into a single decay curve).

Whether the spectral evolution in TMpCA can be entirely attributed to solvation is difficult to answer unequivocally. Similar red-shifting behavior of intramolecular twisting molecules can result from barrierless diffusion-type motion of a population along the excited- and ground-state potentials (Abramavicius et al., 2002; Hamm et al., 1996). Both TMpCA and FAL chromophores exhibit nearly identical spectral evolution dynamics, even though FAL does not have the twisting degree of freedom. From the strong similarities (Fig. 8) between the observed solvation dynamics, we conclude that isomerization in TMpCA does not appreciably contribute to the observed spectral dynamics. This argument is further reinforced by the absence of shifting in the protein samples (Fig. 7), where solvation contributions, if any, are limited to sub-IRF timescales (Changenet-Barret et al., 2000). Alternatively, the observed shifting may be ascribed to excited-state vibrational relaxation; however, this mainly affects the spectral width of the spectra (Zgrablić et al., 2003); comparing the normalized spectra in Fig. 5, we see that the width of the spectra hardly changes in the first 100 fs. Hence, we exclude vibrational relaxation effects in our signals for the free chromophores.

Even though the red-shifting timescales of the free chromophores in solution are similar, the total static Stokes shifts differ greatly: the shift (peak-to-peak) for TMpCA (6000 cm^{-1}) is considerably greater than for FAL (3700 cm^{-1}). Recent Stark experiments suggest that the change in dipole moment upon excitation is much larger for TMpCA than for the locked chromophores and explain the observed larger Stokes shift (Premvardhan et al., 2004). In contrast, no clear shifting of fluorescence is observed in the protein samples. For the WT PYP and E46Q samples, where an isomerization reaction occurs that initiates the protein photocycle (Devanathan et al., 2000), an instrument-limited narrowing of the spectra is discernable (Figs. 3 and 7). This narrowing has been previously observed in fluorescence up-conversion measurements and ascribed to small-scale excited-state reorganization and vibrational relaxation of the molecule (Changenet et al., 1998; Hanada et al., 2001). In contrast, the signals measured from the WTL and E46QL samples exhibit no such narrowing (Fig. 5 B and Fig. 7), suggesting that this component can be ascribed to ultrafast evolution that includes evolution along the twisting coordinate. Alternatively, the ultrafast spectral narrowing can also be ascribed to intramolecular vibrational redistribution of the isomerizing chromophores. For E46Q, the absorption spectrum is more red-shifted, meaning that a larger amount of energy needs to be redistributed than for WT-PYP. We must note that the fact that no dynamic red-shifting of the spectrum is observed in the photoactive proteins does not

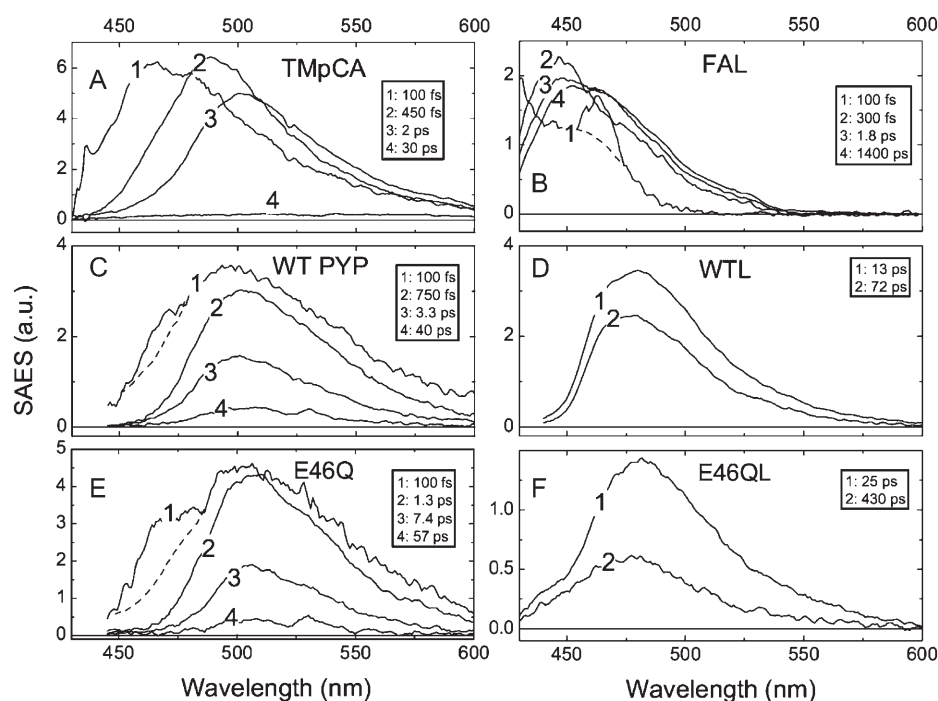


FIGURE 7 Estimated species-associated emission spectra (SAES) from the global analysis based on sequential model. (A) TMpCA; (B) FAL; (C) WT PYP; (D) WTL; (E) E46Q; and (F) E46QL. The time constants associated with each SAES are shown in the legends. Raman and Rayleigh scattering from the solvent partially contaminates the early SAES (1) in some samples (B, D, E, F).

mean that the shifting does not occur; it just indicates that it occurs much faster than our IRF.

Although isomerization does not result in additional spectral shifting, it certainly affects the excited-state lifetime. Although the excited-state dynamics for FAL and TMpCA occurs on multiple timescales, the initial timescales predominately constitute spectral evolution (shifting) and the final timescale describes essentially single-exponential

quenching kinetics (2 ps to TMpCA and >1 ns for FAL). In other words, the largest loss of integrated fluorescence (compare the areas of the SAES in Fig. 7, A and B) can more or less be attributed to a single kinetic step with a specific lifetime. In contrast, the fluorescence signals observed in all protein samples exhibit distinctly multiexponential decays, with the SAES for the different decay timescales exhibiting near identical spectral shapes (Fig. 7). These multiexponential kinetics can be ascribed to different mechanisms: either homogeneous or inhomogeneous with dynamics evolving either sequentially or in parallel, respectively. Within the homogeneous model, the multiexponential behavior is ascribed to inherent nonlinear system dynamics, which may exhibit multiple dynamical timescales because of evolution over a complex energy surface (e.g., including multiple energy barriers). In this model, the observed excited-state twisting in PYP may include effects from the protein relaxation, such as a time-dependent resistance to the twisting motion or a time-dependent dielectric response to the changing dipole moment of the chromophore. Furthermore, if the isomerization is accompanied by a changing fluorescence oscillator strength then combined with the decay kinetics, complex multiexponential kinetics would be observed (Abramavicius et al., 2002; Ruhman et al., 2002). Such torsion-angle dependence of the transition dipole moment has been predicted for the model chromophore of bacteriorhodopsin (Cembran et al., 2003).

However, a more simple model ascribing the multiexponential decay kinetics to the excitation of an inhomogeneous distribution of the protein configurations (or amino-acid configurations or hydrogen-bond strengths) can

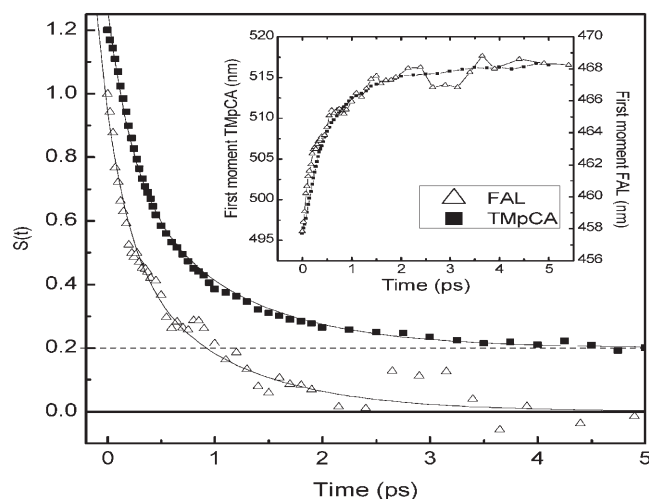


FIGURE 8 Time-resolved Stokes shifts for FAL (open triangles) and TMpCA (solid squares). The plot for TMpCA was offset by 0.2 for clarity. The inset shows the time-dependence of the first spectral moment of the signals. Two-exponential fit to the data is shown as solid lines. The biexponential fitting parameters for both TMpCA and FAL are $A_1 = 0.5$ with $\tau_1 = 225$ fs and $A_2 = 0.5$ with $\tau_2 = 1$ ps.

be proposed, where different subpopulations have different single exponential decay times. Hence, the observed multi-exponential ensemble kinetics constitute a superposition of different kinetics from multiple subpopulations (Gai et al., 1998). In that case, the two orders-of-magnitude difference in the fluorescence decay times (from 750 fs to 40 ps in WT PYP) can hardly be explained if the inhomogeneity would only affect the curvature of the potential energy surfaces in a barrierless model (Fig. 1 A). The situation would be different, though, if a barrier for isomerization existed in the excited state (Fig. 1 B). The height of this barrier would be affected by the structural inhomogeneities and hence the observed differences in isomerization rates would be exponentially modified. Recent quantum calculation on the PYP system suggest that the residues surrounding the chromophore in protein pocket (especially the R52 residue) significantly modulate the ensuing excited-state dynamics (Groenhof et al., 2004). The calculations on the PYP (Groenhof et al., 2004) and the isolated chromophore in solution (Ko et al., 2003) suggest the presence of an excited-state barrier. The sensitivity of the excited-state dynamics to the arrangement of the pigment binding pocket has also been demonstrated experimentally by Mataga et al. (2000a) by investigating different mutants of PYP. Inhomogeneous broadening in PYP has been established by earlier hole-burning experiments (Masciaglioli et al., 2000), whereas the existence of the energy barrier for the isomerization has been suggested by low-temperature fluorescence excitation measurements (Hoff et al., 1992).

Since multiexponential decays are also observed in the WTL and E46QL signals (Fig. 7), where isomerization cannot occur, we suggest that the multiexponential behavior results predominately from the ground-state disorder in the protein environment. This is further supported by the comparison between the decays of FAL and WTL, in which an order-of-magnitude faster quenching is observed for the locked chromophore in the protein environment than in solution (Fig. 4). The interactions between the PYP chromophore and its protein environment, including both covalent and hydrogen bonds with nearby amino-acid residues, enhance the radiationless decay pathways that are not present in the aqueous environment (Larsen et al., 2003, 2004a). The effect of the strength of the hydrogen bond between the E46 residue and the PYP chromophore is obvious from comparison of WTL and E46QL (Fig. 7, D and F). With E46QL, the slowest fluorescence timescale increases sixfold (from 74 ps to 440 ps) upon replacing E46 with the weaker hydrogen-bonding glutamine residue. However, this difference is minor on shorter timescales; the excited-state lifetime in E46Q is only slightly longer than that in WT PYP (Figs. 4 and 7).

The initial decay of fluorescence is *faster* for WT PYP (1 ps) than in TMpCA (2 ps). However, most of the *integrated* (steady-state) fluorescence of WT PYP comes from the *slowly decaying* ~40-ps timescale, which persists for more

than an order-of-magnitude longer than those in TMpCA. Polarization-dependent pump-probe experiments showed that the photochemistry of PYP originates mainly from the fast-decaying excited states (Gensch et al., 2002), which has been reconfirmed by recent dispersed pump-dump-probe results (Larsen et al., 2004b). Thus, the effect of the protein seems to be dual: if the photocycle is initiated, it happens faster than the natural timescale of pigment twisting in solution; however, if the photocycle initiation fails, the protein then acts as a viscous medium and effectively “locks” the pigment, and prolongs the excited-state lifetime. The fact that only the short-lived excited states (<10 ps) initiate the photocycle suggests several possible conclusions. First, the photocycle may be initiated from a “hot” (non-equilibrated with the protein environment) excited state of the pigment. Intermolecular vibrational energy redistribution in proteins has indeed been found to occur on the timescale of several picoseconds (Doig et al., 1991; Kholodenko et al., 2000). Alternatively, a concerted (coherent) protein response may have to take place to use the excited-state energy of the pigment for further photochemistry. This is further supported by the recent up-conversion measurements on PYP and several analogs, where Mataga and co-workers have observed clearly resolved oscillations (Mataga et al., 2002, 2003). These oscillations were ascribed to coherently-excited vibrational wavepacket dynamics that act as promoter modes in initiating the PYP photocycle. Because their data were measured with a better time-resolution than the data presented here, we do not observe these modulations in the signals. However, the fact that the photochemistry is most efficient during the lifetime of vibrational coherence may be an indication that the protein is not only damping the created wavepackets, but also exploiting them for entering the photocycle.

The observed ground-state protein inhomogeneity relates to the second scenario: it is possible that selected possible ground-state configurations of the protein can respond adequately and use the excitation energy for the photochemistry with higher quantum yields than other configurations. Recent *ab initio* calculations support a similar conclusion (Groenhof et al., 2004, 2002a,b). However, it is not possible to answer which precise structural changes in the protein would govern the quantum yield of the photochemistry. The answer to this question may be obtainable from the methods that are more specific to the protein structure, such as time-resolved vibrational spectroscopies.

CONCLUSIONS

We have measured frequency- and time-resolved fluorescence on six samples: wild-type PYP, its E46Q mutant, and hybrids of both containing a locked chromophore, and contrasted these results with signals obtained for native (TMpCA) and locked (FAL) pigments in aqueous solution.

In solution, both the isolated pigments exhibit dynamic spectral shifting of fluorescence with approximately single-exponential decay, whereas in the proteins the fluorescence decay is multiexponential without resolvable spectral shifting. This shifting in solution is attributed mostly to solvation dynamics, and the photoinduced twisting of the pigment is manifested as excited-state quenching, but not as an additional spectral shifting. Time-resolved fluorescence data in WT PYP shows large inhomogeneity in the fluorescence decay rates and essentially no time-dependent red-shifting of the fluorescence, which points toward an isomerization mechanism that includes a small energy barrier in the excited state.

This research was supported by the Netherlands Organization for Scientific Research via the Dutch Foundation for Earth and Life Sciences and by the Swiss National Science Foundation within the National Centres of Competence in Research "Quantum Photonics". D.S.L. is grateful to the Human Frontier Science Program Organization for providing financial support with a long-term fellowship. M.V. received financial support from the Stichting voor Fundamenteel Onderzoek der Materie, Netherlands and the European Science Foundation (ULTRA program). S.H. is grateful for the Swiss National Fund for Scientific Research-PROFIL-2 grant.

REFERENCES

- Abramavicius, D., V. Gulbinas, L. Valkunas, Y.-J. Shiu, K. Liang, M. Hayashi, and S. Lin. 2002. Molecular twisting and relaxation in the excited state of triarylpyrylium cations. *J. Phys. Chem. A*. 106:8864–8869.
- Alfano, R., R. Govindjee, B. Becher, and T. Ebrey. 1976. Picosecond kinetics of the fluorescence from the chromophore of the purple membrane protein of *Halobacterium halobium*. *Biophys. J.* 16:541–545.
- Baca, M., G. E. Borgstahl, M. Boissinot, P. M. Burke, D. R. Williams, K. A. Slater, and E. D. Getzoff. 1994. Complete chemical structure of photoactive yellow protein: novel thioester-linked 4-hydroxycinnamyl chromophore and photocycle chemistry. *Biochemistry*. 33:14369–14377.
- Baltuška, A., I. H. M. van Stokkum, A. Kroon, R. Monshouwer, K. J. Hellingwerf, and R. van Grondelle. 1997. The primary events in the photoactivation of yellow protein. *Chem. Phys. Lett.* 270:263–266.
- Cembran, A., F. Bernardi, M. Olivucci, and M. Garavelli. 2003. Excited-state singlet manifold and oscillatory features of a nonatetraeniminium retinal chromophore model. *J. Am. Chem. Soc.* 125:12509–12519.
- Changenet-Barret, P., H. Zhang, M. J. van der Meer, K. J. Hellingwerf, and M. Glasbeek. 1998. Subpicosecond fluorescence up-conversion measurements of primary events in yellow proteins. *Chem. Phys. Lett.* 282:276–282.
- Changenet-Barret, P., C. Choma, E. Gooding, W. DeGrado, and R. M. Hochstrasser. 2000. Ultrafast dielectric response of proteins from dynamics Stokes shifting of coumarin in calmodulin. *J. Phys. Chem. B*. 104:9322–9329.
- Changenet-Barret, P., A. Espagne, N. Katsonis, S. Charié, J.-B. Baudin, L. Jullien, P. Plaza, and M. M. Martin. 2002. Excited-state relaxation dynamics of a PYP chromophore model in solution: influence of the thioester group. *Chem. Phys. Lett.* 365:285–291.
- Changenet-Barret, P., P. Plaza, and M. M. Martin. 2001. Primary events in the photoactive yellow protein chromophore in solution. *Chem. Phys. Lett.* 336:439–444.
- Cusanovich, M. A., and T. E. Meyer. 2003. Photoactive yellow protein: a prototypic PAS domain sensory protein and development of a common signaling mechanism. *Biochemistry*. 42:4759–4770.
- Devanathan, S., S. Lin, M. A. Cusanovich, N. Woodbury, and G. Tollin. 2000. Early intermediates in the photocycle of the Glu⁴⁶Gln mutant of photoactive yellow protein: femtosecond spectroscopy. *Biophys. J.* 79:2132–2137.
- Devanathan, S., A. Pacheco, L. Uji, M. Cusanovich, G. Tollin, S. Lin, and N. Woodbury. 1999. Femtosecond spectroscopic observations of initial intermediates in the photocycle of the photoactive yellow protein from *Ectothiorhodospira halophila*. *Biophys. J.* 77:1017–1023.
- Doig, S. J., P. J. Reid, and R. A. Mathies. 1991. Picosecond time-resolved resonance Raman spectroscopy of bacteriorhodopsin-J, bacteriorhodopsin-K, bacteriorhodopsin-K1 intermediates. *J. Phys. Chem.* 95:6372–6379.
- Du, M., and G. R. Fleming. 1993. Femtosecond time-resolved fluorescence spectroscopy of bacteriorhodopsin—direct observation of excited-state dynamics in the primary step of the proton pump cycle. *Biophys. Chem.* 48:101–111.
- Gai, F., K. C. Hasson, J. C. McDonald, and P. A. Anfinrud. 1998. Chemical dynamics in proteins: the photoisomerization of retinal in bacteriorhodopsin. *Science*. 279:1886–1891.
- Gai, F., J. C. McDonald, and P. A. Anfinrud. 1997. Pump-dump-probe spectroscopy of bacteriorhodopsin: evidence for a near-IR excited state absorbance. *J. Am. Chem. Soc.* 119:6201–6202.
- Genick, U. K., G. E. Borgstahl, K. Ng, Z. Ren, C. Pradervand, P. M. Burke, V. Srajer, T. Y. Teng, W. Schildkamp, D. E. McRee, K. Moffat, and E. D. Getzoff. 1997. Structure of a protein photocycle intermediate by millisecond time-resolved crystallography. *Science*. 275:1471–1475.
- Gensch, T., C. C. Gradinaru, I. H. M. van Stokkum, J. Hendriks, K. Hellingwerf, and R. van Grondelle. 2002. The primary photoreaction of photoactive yellow protein (PYP): anisotropy changes and excitation wavelength dependence. *Chem. Phys. Lett.* 356:347–354.
- Gonzalez-Luque, R., M. Garavelli, F. Bernardi, M. Merchán, M. A. Robb, and M. Olivucci. 2000. Computational evidence in favor of a two-state, two-mode model of the retinal chromophore photoisomerization. *Proc. Natl. Acad. Sci. USA*. 97:9379–9384.
- Groenhof, G., M. Bouxin-Cademartory, B. Hess, S. de Visser, H. Brendendsen, M. Olivucci, A. E. Mark, and M. A. Robb. 2004. Why photon absorption triggers isomerization of the chromophore in photoactive yellow protein. *J. Am. Chem. Soc.* 126:4228–4233.
- Groenhof, G., M. F. Lensink, H. J. C. Berendsen, and A. E. Mark. 2002a. Signal transduction in the photoactive yellow protein. I. Proton transfer initiates conformational changes. *Proteins Struct. Funct. Gen.* 48:212–219.
- Groenhof, G., M. F. Lensink, H. J. C. Berendsen, J. G. Snijders, and A. E. Mark. 2002b. Signal transduction in the photoactive yellow protein. I. Photon absorption and the isomerization of the chromophore. *Proteins Struct. Funct. Gen.* 48:202–211.
- Groot, M. L., L. van Wilderen, D. S. Larsen, M. A. van der Horst, I. H. M. van Stokkum, K. J. Hellingwerf, and R. van Grondelle. 2003. Initial steps of signal generation in photoactive yellow protein revealed with femtosecond mid-infrared spectroscopy. *Biochemistry*. 42:10054–10059.
- Haacke, S., R. A. Taylor, I. Bar-Joseph, M. Brasil, M. Hartig, and B. Deveaud. 1998. Improving the signal-to-noise ratio of femtosecond luminescence up-conversion by multichannel detection. *J. Optic. Soc. Am. B Optic. Phys.* 15:1410–1417.
- Hamm, P., M. Zurek, T. Röscher, H. Patselt, D. Oesterhelt, and W. Zinth. 1996. Femtosecond spectroscopy of the photoisomerization of the protonated Schiff base of all-trans retinal. *Chem. Phys. Lett.* 263:613–621.
- Hanada, H., Y. Kanematsu, S. Kinoshita, M. Kumauchi, J. Sasaki, and F. Tokunaga. 2001. Ultrafast fluorescence spectroscopy of photoactive yellow protein. *J. Luminesc.* 94:593–596.
- Hasson, K. C., F. Gai, and P. A. Anfinrud. 1996. The photoisomerization of retinal in bacteriorhodopsin: experimental evidence for a three-state model. *Proc. Natl. Acad. Sci. USA*. 93:15124–15129.

- Hellingwerf, K. J., J. Hendriks, and T. Gensch. 2003. Photoactive yellow protein, a new type of photoreceptor protein: will this "yellow lab" bring us where we want to go? *J. Phys. Chem. A*. 107:1082–1094.
- Hoff, W. D., S. L. S. Kwa, R. van Grondelle, and K. J. Hellingwerf. 1992. Low temperature absorbance and fluorescence spectroscopy of the photoactive yellow protein from *Ectothiorhodospira halophila*. *Photochem. Photobiol.* 56:529–539.
- Hoff, W. D., I. H. M. van Stokkum, H. J. van Ramesdonk, M. E. van Brederode, A. M. Brouwer, J. C. Fitch, T. E. Meyer, R. van Grondelle, and K. J. Hellingwerf. 1994. Measurement and global analysis of the absorbance changes in the photocycle of the photoactive yellow protein from *Ectothiorhodospira halophila*. *Biophys. J.* 67:1691–1705.
- Holzwarth, A. R. 1996. Data analysis in time-resolved measurements. In *Biophysical Techniques in Photosynthesis*. J. Ames and A. J. Hoff, editors. Kluwer, Dordrecht, The Netherlands.
- Humphrey, W., H. Lu, I. Logunov, H. J. Werner, and K. Schulten. 1998. Three electronic state model of the primary phototransformation of bacteriorhodopsin. *Biophys. J.* 75:1689–1699.
- Imamoto, Y., M. Kataoka, F. Tokunaga, T. Asahi, and H. Masuhara. 2001. Primary photoreaction of photoactive yellow protein studied by subpicosecond-nanosecond spectroscopy. *Biochemistry*. 40:6047–6052.
- Jarzeba, W., G. C. Walker, A. E. Johnson, and B. F. Barbara. 1991. Nonexponential solvation dynamics of simple liquids and mixtures. *Chem. Phys.* 152:57–68.
- Jimenez, R., G. R. Fleming, P. V. Kumar, and M. Maroncelli. 1994. Femtosecond solvation dynamics of water. *Nature*. 369:471–473.
- Kholodenko, Y., M. Volk, E. Gooding, and R. M. Hochstrasser. 2000. Energy dissipation and relaxation processes in deoxy myoglobin after photoexcitation in the Soret region. *Chem. Phys.* 259:71–87.
- Ko, C., B. Levine, A. Toniolo, L. Monohar, S. Olsen, H.-J. Werner, and T. J. Martinez. 2003. Ab initio excited-state dynamics of the photoactive yellow protein chromophore. *J. Am. Chem. Soc.* 125:12710–12711.
- Kort, R., W. D. Hoff, M. Van West, A. R. Kroon, S. M. Hoffer, K. H. Vlieg, W. Crielaand, J. J. Van Beeumen, and K. J. Hellingwerf. 1996. The xanthopsins: a new family of eubacterial blue-light photoreceptors. *EMBO J.* 15:3209–3218.
- Kort, R., M. K. Phillips-Jones, D. M. van Aalten, A. Haker, S. M. Hoffer, K. J. Hellingwerf, and W. Crielaand. 1998. Sequence, chromophore extraction and 3-D model of the photoactive yellow protein from *Rhodobacter sphaeroides*. *Biochim. Biophys. Acta*. 1385:1–6.
- Larsen, D. S., M. Vengris, I. H. M. van Stokkum, M. van der Horst, R. Cordfunke, K. J. Hellingwerf, and R. van Grondelle. 2003. Initial photoinduced dynamics of the photoactive yellow protein chromophore in solution. *Chem. Phys. Lett.* 369:563–569.
- Larsen, D. S., M. Vengris, I. H. M. van Stokkum, M. van der Horst, F. L. de Weerd, K. J. Hellingwerf, and R. van Grondelle. 2004a. Photoisomerization and photoionization of the photoactive yellow protein chromophore in solution. *Biophys. J.* 86:2538–2550.
- Larsen, D., I. H. M. van Stokkum, M. Vengris, M. A. van der Horst, F. L. de Weerd, K. J. Hellingwerf, and R. van Grondelle. 2004b. Incoherent manipulation of the photoactive yellow protein photocycle with dispersed pump-dump-probe spectroscopy. *Biophys. J.* 87:1858–1872.
- Masciaglioli, T., S. Devanathan, M. A. Cusanovich, G. Tollin, and M. A. El-Sayed. 2000. Probing the primary event in the photocycle of photoactive yellow protein using photochemical hole-burning technique. *Photochem. Photobiol.* 72:639–644.
- Mataga, N., H. Chosrowjan, Y. Shibata, Y. Imamoto, M. Kataoka, and F. Tokunaga. 2002. Ultrafast photoinduced reaction dynamics of photoactive yellow protein (PYP): observation of coherent oscillations in the femtosecond fluorescence decay dynamics. *Chem. Phys. Lett.* 352:220–225.
- Mataga, N., H. Chosrowjan, Y. Shibata, Y. Imamoto, and F. Tokunaga. 2000a. Effects of modification of protein nanospace structure and change of temperature on the femtosecond to picosecond fluorescence dynamics of photoactive yellow protein. *J. Phys. Chem. B*. 104:5191–5199.
- Mataga, N., H. Chosrowjan, Y. Shibata, Y. Imamoto, F. Tokunaga, and F. Tanaka. 2000b. Femtosecond fluorescence studies on ultrafast reaction dynamics of photoactive proteins. *J. Luminesc.* 98–89:821–823.
- Mataga, N., H. Chosrowjan, S. Taniguchi, N. Hamada, F. Tokunaga, Y. Imamoto, and M. Kataoka. 2003. Ultrafast photoreactions in protein nanospaces as revealed by femtosecond fluorescence dynamics measurements on photoactive yellow protein and related systems. *Phys. Chem. Chem. Phys.* 5:2454–2460.
- Perman, B., V. Srajer, Z. Ren, T. Teng, C. Pradervand, T. Ursby, D. Bourgeois, F. Schotte, M. Wulff, R. Kort, K. Hellingwerf, and K. Moffat. 1998. Energy transduction on the nanosecond time scale: early structural events in a xanthopsin photocycle. *Science*. 279:1946–1950.
- Premvardhan, L. L., F. Buda, M. A. van der Horst, D. Luehrs, K. J. Hellingwerf, and R. van Grondelle. 2004. The impact of photon absorption on the electronic properties of p-coumaric acid derivatives of the photoactive yellow protein chromophore. *J. Phys. Chem. B*. 108:5138–5148.
- Ren, Z., B. Perman, V. Srajer, T.-V. Teng, C. Pradervand, D. Bourgeois, F. Schotte, T. Ursby, R. Kort, M. Wulff, and K. Moffat. 2001. A molecular movie at 1.8 Å resolution displays the photocycle of photoactive yellow protein, a eubacterial blue-light receptor, from nanoseconds to seconds. *Biochemistry*. 40:13788–13801.
- Rubinstenn, G., G. W. Vuister, F. A. Mulder, P. E. Dux, R. Boelens, K. J. Hellingwerf, and R. Kaptein. 1998. Structural and dynamic changes of photoactive yellow protein during its photocycle in solution. *Nat. Struct. Biol.* 5:568–570.
- Ruhman, S., B. Hou, N. Freidman, M. Ottolenghi, and M. Sheves. 2002. Following evolution of bacteriorhodopsin in its reactive excited state via stimulated emission pumping. *J. Am. Chem. Soc.* 124:8854–8858.
- Sprenger, W. W., W. D. Hoff, J. P. Armitage, and K. J. Hellingwerf. 1993. The eubacterium *Ectothiorhodospira halophila* is negatively phototactic, with a wavelength dependence that fits the absorption spectrum of the photoactive yellow protein. *J. Bacteriol.* 175:3096–3104.
- van Beeumen, J. J., B. V. Devreese, S. M. van Bun, W. D. Hoff, K. J. Hellingwerf, T. E. Meyer, D. E. McRee, and M. A. Cusanovich. 1993. Primary structure of a photoactive yellow protein from the phototrophic bacterium *Ectothiorhodospira halophila*, with evidence for the mass and the binding site of the chromophore. *Protein Sci.* 2:1114–1125.
- van Brederode, M. E., W. D. Hoff, I. H. Van Stokkum, M. L. Groot, and K. J. Hellingwerf. 1996. Protein folding thermodynamics applied to the photocycle of the photoactive yellow protein. *Biophys. J.* 71:365–380.
- Xie, A., L. Kelemen, J. Hendriks, B. J. White, K. J. Hellingwerf, and W. D. Hoff. 2001. Formation of a new buried charge drives a large-amplitude protein quake in photoreceptor activation. *Biochemistry*. 40:1510–1517.
- Zgrablić, G., K. Votchkovsky, M. Kindermann, M. Chergui, and S. Haacke. 2003. Ultrafast photophysics of the protonated Schiff base of retinal in alcohols studied by femtosecond fluorescence up-conversion. In *Femtochemistry and Femtobiology: Ultrafast Events in Molecular Science*. M. M. Martin and J. T. Hynes, editors. Elsevier, Paris, France.